

The 120^0 ordered phase of the spin-1 J_1 - J_2 antiferromagnetic Heisenberg model on a triangular lattice

Nguyen Van Hinh^{1,†}, Pham Thi Thanh Nga² and Nguyen Toan Thang³

¹*Hanoi University of Industry,
298 Cau Dien, Bac Tu Liem, Hanoi, Vietnam*

²*Faculty of Electrical and Electronics Engineering, Thuyloi University,
175 Tay Son, Dong Da, Hanoi, Vietnam*

³*Institute of Physics, Vietnam Academy of Science and Technology,
10 Dao Tan, Ba Dinh, Hanoi 11108, Vietnam*

E-mail: [†]nguyen.hinh@hau.edu.vn

Received 26 November 2022

Accepted for publication 8 May 2023

Published 31 May 2023

Abstract. *We study the effect of quantum and thermal fluctuations on the excitation energy spectrum and sublattice magnetization of the 120^0 ordered phase of the spin-1 antiferromagnetic Heisenberg model on a triangular lattice with nearest- J_1 and next-nearest-neighbor J_2 exchange interactions. The auxiliary fermionic representation of the spin operators within a functional integral formalism with an imaginary Lagrange multiplier is employed to retain an exact constraint of single particle occupancy. Representing the classical ground state by Luttinger-Tisza ordering vector \mathbf{Q} one may consider the fluctuation contributions to the free energy of the system in the entire range of the coupling parameters. We derived the magnon spectrum in one-loop approximation and the magnetization taking into account thermal fluctuations. The obtained results are compared with the result of the linear spin-wave approximation and experimental findings on compound NiGa_2S_4 .*

Keywords: strongly correlated electron systems; antiferromagnetics; Heisenberg model; triangular lattice.

Classification numbers: 71.27.+a; 75.10.Jm; 75.50.Ee.

©2023 Vietnam Academy of Science and Technology

1. Introduction

The antiferromagnetic Heisenberg model on a triangular lattice with nearest- J_1 and next-nearest-neighbor J_2 exchange interactions has been extensively studied from both the theoretical and experimental viewpoints in recent years because it is a typically example for a geometrically frustrated spin system. In general, quantum fluctuations will be largest for the case spin $s = 1/2$, and that they will reduce to zero as $s \rightarrow \infty$. For this reason spin-1/2 magnets attract the greatest attention. For the spin-1/2 antiferromagnetic Heisenberg model, at the classical level, the ground state of the system has three different types of structures depending on the value of the ratio $\alpha = J_2/J_1$ of couplings. For values $-\infty < \alpha \leq 1/8$, this system is known to take a well-known 120° structure in which the lattice is divided into three sublattices that neighboring spin are oriented 120° relative to each other; while for $1/8 < \alpha < 1$ the ground states become degenerate into any four-sublattice states that satisfy $\mathbf{S}_1 + \mathbf{S}_2 + \mathbf{S}_3 + \mathbf{S}_4 = 0$, where \mathbf{S}_i denotes the spin at sublattice site i ; and when $\alpha > 1$, the system has an incommensurate spin structure [1]. When one investigates the properties of ground states and phase transitions, a open question arises as to whether or not the combined effect of quantum fluctuations and geometrical frustration that present in the lattice destroy long-range Néel type order. The spin-wave theory [1-5] predicts that quantum fluctuations on the spin-1/2 triangular-lattice are insufficient to suppress the classical Néel order, but lead to a reduction in the sublattice magnetization of around 50% from its classical value. While many of the numerical studies [6-9] based on the exact diagonalization of small lattice clusters predicted that the ground state has very small or zero magnetic long-range order (LRO). Some calculations [10-13] conjecture the absence of a sublattice LRO, instead a disordered state like the spin-liquid state, others [14, 15] suggest a quasiclassical ordered state. The controversial results gives an indication that the problem has not been theoretically resolved yet.

In contrast to the $s = 1/2$, the conclusive results for the $s = 1$ antiferromagnetic Heisenberg model in this geometrical frustration are scarce. On the one hand due to the lack of experimental data, on the other hand powerful numerical techniques (e.g. density-matrix renormalization group) cannot be easily applied for this model. The active interest in the model was revived recently by the unconventional magnetic properties observed in the Ni-based compound NiGa_2S_4 [16]. In this material, spin-1 carrying Ni^{2+} ions reside on weakly coupled triangular lattice layers. NiGa_2S_4 demonstrates a spin disorder down to the temperature $T \approx 0.35\text{K}$, incommensurate short-range spin correlations and a quadratic low-temperature dependence of the specific heat.

In this work we study the spin-1 antiferromagnetic Heisenberg model on a triangular lattice with nearest- J_1 and next-nearest-neighbor J_2 exchange interactions. Similarly the linear spin wave approximation, it starts from the assumption that Néel order exists, and then the physical quantities found must be self-consistent with assumption. Here, we also assume that the 120° Néel ordered phase of Heisenberg antiferromagnet triangular lattice with long range couplings exists. We use Popov-Fedotov (PF) functional integral formalism and Luttinger-Tisza procedure representing the classical ground state to consider the fluctuation contributions to the free energy of the system [17]. We derived the magnon spectrum, sublattice magnetization, and study their temperature dependence in a mean field approach within the one-loop approximation. The obtained results is compared with the result of the linear spin-wave (LSW) approximation and experimental findings on compound NiGa_2S_4 .

The remainder of this article is organized as follows: In Section 2 we present the derivation of the partition function under the single particle site occupation constraint. The mean-field and first order loop expansion term contributions are derived in Section 3. In Section 4 we determine sublattice magnetization and one-magnon excitation spectrum, and discuss the results obtained at the different levels of approximation. Comments are presented and conclusions are drawn in Section 5. Some of the analytical results reported in this work have been partially reported in the proceedings of the Vietnam conference on theoretical physics [18].

2. Model and formalism

We start with the Hamiltonian

$$H = J_1 \sum_{\langle ij \rangle} \mathbf{S}_i \mathbf{S}_j + J_2 \sum_{\langle\langle kl \rangle\rangle} \mathbf{S}_k \mathbf{S}_l, \quad (1)$$

where \mathbf{S}_i represents a spin located at site i , and $\langle ij \rangle$, $\langle\langle kl \rangle\rangle$ denote the sum extends over all nearest-neighbor (NN) sites, and next-nearest-neighbor (NNN) sites, respectively.

We shall be interested here only in the case of competing or frustrating antiferromagnetic bonds $J_1 > 0$, $J_2 > 0$ and $J_2 = \alpha J_1$ where $0 \leq \alpha \leq 0.125$. All energies will be given in the unit of J_1 .

Firstly, we brief some analytically results found out in the early publication [18]. In that work we considered a general antiferromagnetic Heisenberg Hamiltonian on a Bravais lattice given by

$$H = \sum_{ij} J_{ij} \mathbf{S}_i \mathbf{S}_j, \quad (2)$$

where \mathbf{S}_i denotes the $S = 1$ spin vector operator and $J_{ij} > 0$ which is antiferromagnetic interaction between the sites.

Applying PF method to spin systems with $S = 1$ we have obtained the analytical expressions for the mean - field magnetization under the constraint of strict single site occupancy, magnetization taking into account thermal and quantum fluctuations, and magnon spectrum as follows

$$m_0 = -\frac{2 \sinh(-\beta \lambda m_0)}{1 + 2 \cosh(-\beta \lambda m_0)}, \quad (3)$$

$$m = m_0 + \delta m_{zz} + \delta m_{+-}, \quad (4)$$

$$\begin{cases} E(\mathbf{k}) &= \lambda m_0 \omega(\mathbf{k}) \\ \omega^2(\mathbf{k}) &= \left(1 - \frac{X(\mathbf{k})}{\lambda}\right) \left(1 - \frac{Y(\mathbf{k})}{\lambda}\right). \end{cases} \quad (5)$$

Here $\beta = 1/(k_B T)$ is the inverse temperature, $\omega(\mathbf{k})$ is the frequency of the spin excitations, δm_{zz} and δm_{+-} which are the fluctuating contributions to the longitudinal and transverse parts of the magnetization respectively given by

$$\delta m_{zz} = -\frac{1}{2N} \sum_{\mathbf{k}} \frac{1}{A_0(\mathbf{k})} \left\{ \left(\frac{W^2(\mathbf{k})}{X(\mathbf{k}) - \lambda} + X(\mathbf{k}) \right) m_0 \Delta m \beta \left(2 - \frac{1}{\sqrt{4 - 3m_0^2}} \right) + \frac{W^2(\mathbf{k}) K_2^{zz}}{m_0 (X(\mathbf{k}) - \lambda)^2} \right\}, \quad (6)$$

$$\delta m_{+-} = -\frac{1}{2N} \sum_{\mathbf{k} \in \text{BZ}} \coth\left(\frac{\beta E(\mathbf{k})}{2}\right) \left[\Delta m \cdot \lambda \cdot \omega(\mathbf{k}) + \frac{1 - \frac{X(\mathbf{k}) + Y(\mathbf{k})}{2\lambda}}{\omega(\mathbf{k})} \right] + \frac{1}{2} (1 + \lambda \cdot \Delta m) \coth\frac{\beta \lambda m_0}{2}, \quad (7)$$

with N is number of lattice sites,

$$\begin{aligned} A_0(\mathbf{k}) &= \left(\frac{W^2(\mathbf{k})}{X(\mathbf{k}) - \lambda} + X(\mathbf{k}) \right) K_2^{zz} + 1, \\ K_2^{zz} &= -\beta \left[\frac{(1 - m_0^2) \sqrt{4 - 3m_0^2}}{1 + \sqrt{4 - 3m_0^2}} \right], \\ \Delta m &= \frac{-K_2^{zz}}{1 + \lambda K_2^{zz}}, \\ \lambda &= -\sum_{\boldsymbol{\delta}_i} J_{\boldsymbol{\delta}_i} \cos(\mathbf{Q} \cdot \boldsymbol{\delta}_i), \end{aligned} \quad (8)$$

and $X(\mathbf{k}), Y(\mathbf{k}), W(\mathbf{k})$ are the components of the exchange interaction after Fourier transformation

$$\begin{cases} X(\mathbf{k}) &= -\sum_{\boldsymbol{\delta}_i} J_{\boldsymbol{\delta}_i} \cos(\mathbf{k} \cdot \boldsymbol{\delta}_i) \cos(\mathbf{Q} \cdot \boldsymbol{\delta}_i) \\ Y(\mathbf{k}) &= -\sum_{\boldsymbol{\delta}_i} J_{\boldsymbol{\delta}_i} \cos(\mathbf{k} \cdot \boldsymbol{\delta}_i) \\ W(\mathbf{k}) &= i \sum_{\boldsymbol{\delta}_i} J_{\boldsymbol{\delta}_i} \sin(\mathbf{k} \cdot \boldsymbol{\delta}_i) \sin(\mathbf{Q} \cdot \boldsymbol{\delta}_i) \end{cases} \quad (9)$$

$\sum_{\boldsymbol{\delta}_i}$ denote the sum extends over all nearest-neighbor and next nearest-neighbor sites, $J_{\boldsymbol{\delta}_i} = J_1 \sum_{\boldsymbol{\delta}^{(1)}} \delta_{i, j+\boldsymbol{\delta}^{(1)}} + J_2 \sum_{\boldsymbol{\delta}^{(2)}} \delta_{i, j+\boldsymbol{\delta}^{(2)}}$ with the vectors $\boldsymbol{\delta}^{(1)}$ and $\boldsymbol{\delta}^{(2)}$ connecting the NN and NNN sites.

We now focus on Hamiltonian (1). In the general frustrated lattice described by Hamiltonian (1) the classical ground states have long range order, which may be parametrized by some magnetic ordering vector \mathbf{Q} . We assume that the spins are planar in the plane Oxz and are described as follows:

$$\mathbf{S}_i = S(\mathbf{u} \cdot \sin \mathbf{Q} \cdot \mathbf{r}_i + \mathbf{v} \cdot \cos \mathbf{Q} \cdot \mathbf{r}_i), \quad (10)$$

where \mathbf{u}, \mathbf{v} are unit vectors along Ox and Oz axes respectively, \mathbf{r}_i is the position vector of site i . Then the vector \mathbf{Q} defines the relative orientation of the spins on the lattice. Namely, an angle between the vectors \mathbf{S}_i and \mathbf{S}_j is given by:

$$\theta_{ij} = \theta_i - \theta_j = \mathbf{Q} \cdot (\mathbf{r}_i - \mathbf{r}_j). \quad (11)$$

The classical energy which is represented in terms of the ordering vector \mathbf{Q} read

$$E_{cl} = \frac{1}{2} N S^2 J(\mathbf{Q}), \quad (12)$$

where $J(\mathbf{k})$ is the Fourier transform of J_{ij} and has form

$$\begin{aligned}
 J(\mathbf{k}) &= J_1 \sum_{\delta_i^{(1)}} e^{i\mathbf{k}\delta_i^{(1)}} + \alpha J_1 \sum_{\delta_i^{(2)}} e^{i\mathbf{k}\delta_i^{(2)}} \\
 &= 2J_1 \left\{ \cos k_x + 2 \cos \frac{k_x}{2} \cos \frac{\sqrt{3}k_y}{2} + \alpha \left[\cos(\sqrt{3}k_y) + 2 \cos\left(\frac{3}{2}k_x\right) \cos\left(\frac{\sqrt{3}}{2}k_y\right) \right] \right\}. \quad (13)
 \end{aligned}$$

Classical ground state can be found by minimizing (12) with the relaxed constraint on the spin value

$$\sum_{i=1}^N \mathbf{S}_i^2 = NS^2. \quad (14)$$

Differentiating (13) with respect to k_x, k_y we have obtained the various minima of the function $J(\mathbf{k})$ inside the first Brillouin zone of the triangular lattice as α is varied. When $0 \leq \alpha < 1/8$, the $J(\mathbf{k})$ has minimum at six points which are at the corners of the hexagonal Brillouin zone, such as the point with coordinate $\mathbf{Q}_1 = (4\pi/3, 0)$. The system has three-sublattice 120° coplanar order. For $1/8 < \alpha < 1$, the minima of $J(\mathbf{k})$ occur at the centers of the faces such as the point $\mathbf{Q}_2 = (0, 2\pi/\sqrt{3})$. The system is in a collinear state with four-sublattice periodicity, in which the only constraint is to have the four spins sum to zero. When $\alpha > 1$, the minima are located at points which have coordinate $(0, \frac{2}{\sqrt{3}} \arccos(-1/2 - 1/2\alpha))$. It has now generic incommensurate spiral structures.

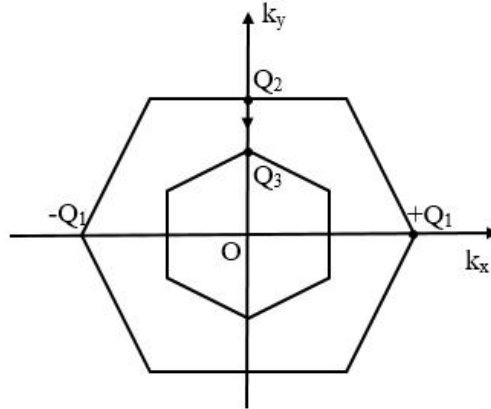


Fig. 1. The Brillouin zone of the triangular lattice. The arrows indicate the path which the Bragg vector \mathbf{Q} of the ground state configuration takes when α increases: $\mathbf{Q} = \mathbf{Q}_1 = (\frac{4\pi}{3}, 0)$ for $-\infty < \alpha < 1/8$; $\mathbf{Q} = \mathbf{Q}_2 = (0, \frac{2\pi}{\sqrt{3}})$ for $1/8 < \alpha < 1$; for $\alpha > 1$ \mathbf{Q} moves continuously from \mathbf{Q}_2 towards $\mathbf{Q}_3 = (0, \frac{4\pi}{3\sqrt{3}})$ at the corner of the $\sqrt{3} \times \sqrt{3}$ Brillouin zone.

In the next section we will treat the ground state of the system as a Néel state to perform numerical calculations for the sublattice magnetization m and the excitation energy spectrum E in the entire range of the coupling parameters $0 \leq \alpha \leq 0.125$. This result describes the effect of quantum and thermal fluctuations on the excitation energy spectrum and sublattice magnetization of the 120° ordered phase of the spin-1 antiferromagnetic Heisenberg model on a triangular lattice.

3. Results and discussion

Firstly, we consider the zero temperature limit ($T \rightarrow 0$). From Eq.(3) we find out the mean - field magnetization under the strict constraint of single site occupancy as $m_0 = 1$. Then the magnetization (4) is reduced to

$$m = \frac{3}{2} - \frac{1}{2N} \sum_{\mathbf{k} \in BZ} \frac{1}{\omega(\mathbf{k})} \left[1 - \frac{(X(\mathbf{k}) + Y(\mathbf{k}))}{2\lambda} \right]. \quad (15)$$

The numerical result of Eq. (15) shows that the magnetization taking into account quantum fluctuations is reduced in comparison with the classical value. We have obtained $m = 0.738703$ for $\alpha = 0$ (this result is a good agreement with the spin-wave result of Miyake [2] and Chernyshev [3], and the large-S expansion result of Chubukov [4]), and m decreases to nearly $m = 0.207699$ for $\alpha = 0.12499$. The $m - \alpha$ phase diagram of the model (1) is outlined on the basis of numerically calculations and shown in Fig. 2.

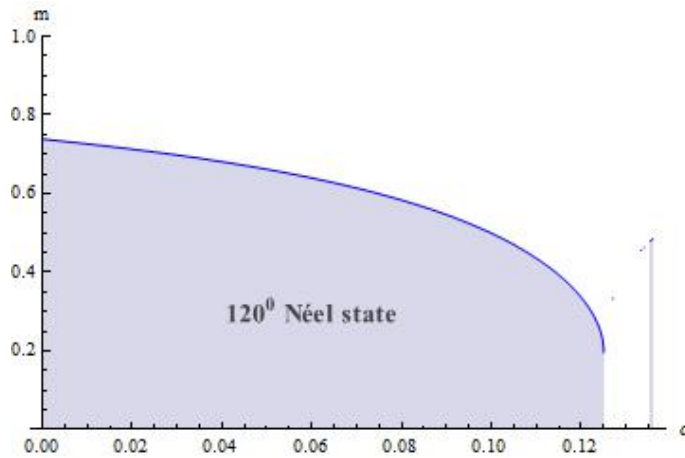


Fig. 2. The sublattice magnetisation m as a function α at $t = 0$.

Figure 2 depicting the dependence of m on α shows that, the system has two phase transitions observed at nearly point $\alpha_1 \approx 0.12499$ and $\alpha_2 \approx 0.135$. This is different from the classical case, in which the system transitions from the 120° Néel state into the collinear state at $\alpha_c = 0.125$. Our result shows that in the interval $0.12499 < \alpha < 0.135$ the system is in a new ground state with no magnetic order. The appearance of this new phase was confirmed in Refs. [10-13], and we will not mention it here.

Let us now discuss about the scaled temperature dependence t ($t = k_B T / J_1$) of the sublattice magnetization and the one-magnon excitation spectrum. The energy spectrum of the magnon at temperature $t = 0$ and $t > 0$ is plotted in Fig. 3.

Fig. 3a shows the spectrum of spin excitations in case of $J_2 = 0$. The frequencies of spin excitations vanish at $\mathbf{k} = 0$ and $\mathbf{k} = \pm \mathbf{Q}_1$, where $\mathbf{Q}_1 = (\frac{4\pi}{3}, 0)$ and $(\pm \frac{2\pi}{3}, \frac{2\pi}{\sqrt{3}})$ are the ordering wavevectors. Therefore, at $t = 0$ the system has LRO, which manifests itself in vanishing frequencies of spin excitations at nonzero ordering vectors (two of these vectors are indicated in Fig. 1;

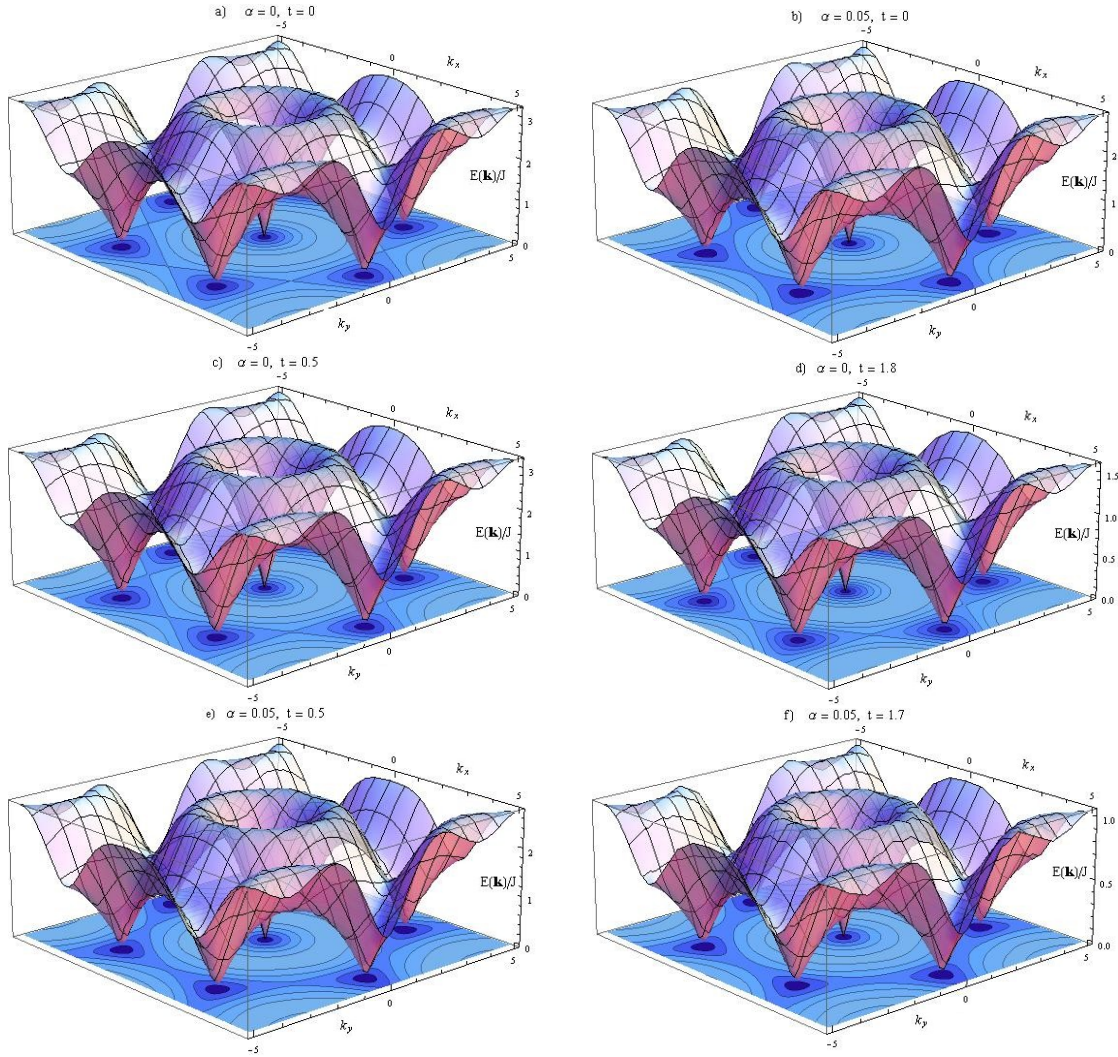


Fig. 3. The spin excitation spectrum $E(\mathbf{k})$ for different values of the frustration parameter α at $t = 0$ and $t \neq 0$.

other four vectors placed at the corners of the first Brillouin zone). These vectors correspond to the mentioned 120^0 spin structure. Thus the ground state of the $S = 1$ model with NN interactions is characterized by the LRO.

The evolution of the zero-temperature spin-excitation spectrum with α is shown in Fig. 3b. In the range of $0 \leq \alpha \leq 0.125$ the frequency of spin excitations vanishes at wave vectors \mathbf{Q}_1 and the dispersion is close to that shown in Fig. 3a. Thus the system retains the 120^0 Néel LRO in this range. A typical dispersion in this range is shown in Fig. 3b.

In Fig. 4 we plot the mean field magnetization m_0 . From the curves of magnetization one can see that in the low temperature region ($t < 0.5$) two curves coincide and are almost invariant ($m_0 = 1$). They are only significantly different in the higher temperature region. At mean-field

level the critical temperature for the exact constraint case (PF theory) is higher than that for average constraint one (LSW theory). This is due to thermal fluctuations into unphysical spinless state in the case of global constraint, which reduce the magnetic moment.

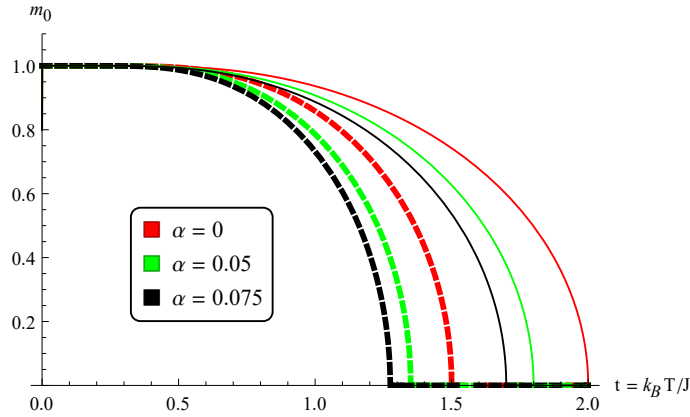


Fig. 4. Temperature dependence of mean field magnetization m_0 for Néel state with $\alpha = 0$; $\alpha = 0.05$ and $\alpha = 0.075$. Dashed line: average-constraint, full line: exact-constraint.

The temperature dependence of one-magnon excitation spectrum is shown in Fig. 3(c,d,e,f). In the low temperature region $t < 0.5$, the energy spectrum is almost unchanged. In the temperature region near the critical temperature, the one-magnon excitation spectrum changes significantly but remains the same form. This is due to the fact that the magnon spectrum given by expression (5) at zero temperature and temperature t differs only by the multiplier $m_0(t)$.

Figure 5 shows the dependence on temperature t and the coupling parameter α of the sublattice magnetization m taking into account effects of fluctuations. At a fixed temperature below the critical temperature, the magnetization is greatest for $\alpha = 0$, and it will decrease as α increases. For $t = 0$ the curve $m(\alpha, t = 0)$ is farthest from the bottom surface, when t is larger, the curve $m(\alpha, t)$ is closer to the bottom surface. This means 120° Néel ordered phase domain shrinks closer to the origin on the parameter axis α (also see Fig. 2). At a fixed frustrated parameter α , the sublattice magnetization m decreases rapidly with increasing temperature. For $\alpha = 0$ the curve $m(\alpha = 0, t)$ is farthest from the horizontal axis, and critical temperature is the biggest. For α is larger, the curve $m(\alpha, t)$ is closer to the bottom surface, which means the lower the critical temperature. In particular, the critical temperature of the lattice magnetization taking into account the influence of fluctuations $t_{c(fl)}$ is very small compared to the one of mean field magnetization $t_{c(mf)}$, for example for $\alpha = 0.05$ then $t_{c(fl)} \approx 0.225$, $t_{c(mf)} \approx 1.799$; for $\alpha = 0.075$ then $t_{c(fl)} \approx 0.177$, $t_{c(mf)} \approx 1.696$. Figure 5 also indicates that temperature t increases over critical temperature, sublattice magnetization $m = 0$. So the maximum critical temperature of the Néel order phase 120° is $t_N = 0.345$ corresponding to $\alpha = 0$.

The above results demonstrate that the considered Heisenberg model has an LRO phase with 120° Néel ordered structure. The quantum fluctuations associated with geometric frustration have a great effect on the Néel ordered phase. Although it does not break this structure, it reduces the energy of the excited states and the sublattice magnetization. Taking into account the influence

of thermal fluctuations, the sublattice magnetization m declines very rapidly with temperature, simultaneously, the value domain of the frustrated parameter shrinks, i.e. the system transforms 120° Néel phase into new phase at a value of the frustration parameter $\alpha_0 < \alpha_c = 0.125$, where α_0 depends on temperature. This is very different from the classical case where the system transitions at the value $\alpha_c = 0.125$.

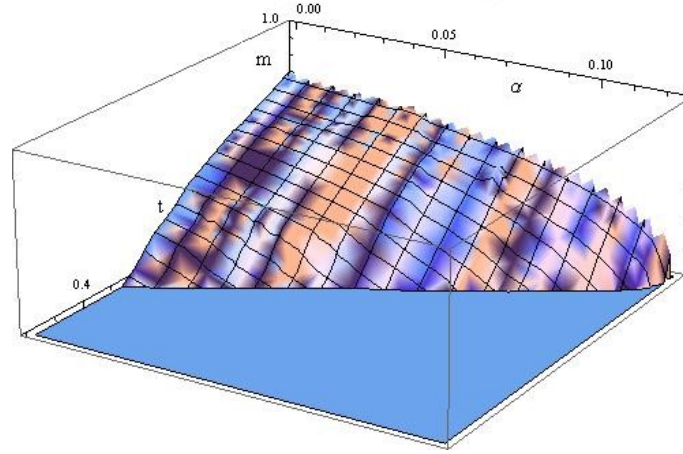


Fig. 5. Temperature and frustrated coupling parameter dependence of one-loop corrected magnetization m .

4. Conclusions

In this work, we have derived the magnon spectrum in the one-loop approximation and the magnetization taking into account the thermal fluctuations. At zero temperature the competition of interactions leads to the appearance a new phase which has no magnetic order between two classical phases. The quantum fluctuations are insufficient to suppress the classical Néel order, but lead to a reduction in the sublattice magnetization of around 26.13% – 79.23% from its classical value. At low temperature the magnon spectrum is almost unchanged, and the magnetization is close to the spin wave value as expected, also in agreement with the previous works [2-4]. As the temperature increases, the thermal fluctuations together with the quantum fluctuations cause the sublattice magnetization m to decrease rapidly. When the temperature approaches the critical temperature T_N , the the sublattice magnetization m approaches 0. We find critical temperature $T_N \approx 0.345J_1/k_B K$ for $\alpha = 0$. When temperature t increases over critical temperature, sublattice magnetization $m = 0$, it means that no magnetic long-range order is observed above this temperature. This result is consistent with specific heat data indicating a disordered low-temperature state without conventional antiferromagnetic order on the compound NiGa_2S_4 [16].

In the present work we aim to work out the expression of the magnon spectrum and the magnetization starting from a specific mean field ansatz and include contribution up to first order in a loop expansion in order to investigate the effect of fluctuation corrections to mean field effects at Gaussian approximation. To complete the magnetic property picture of the new synthesised layered materials containing Ni^{2+} ions, one need to include the third order interaction J_3 . It will be our future study.

Acknowledgements

This research is funded by National Foundation of Science and Technology Development (NAFOSTED) under Grant No. 103.01-2020.20.

References

- [1] Th. Jolicoeur and J. C. Le Guillou, *Spin-wave results for the triangular Heisenberg antiferromagnet*, Phys. Rev. B **40** (1989) 2727.
- [2] S. J. Miyake, *Spin-wave results for the staggered magnetization of triangular Heisenberg antiferromagnet*, J. Phys. Soc. Jpn. **61** (1992) 983.
- [3] A. V. Chubukov, S. Sachdev and T. Senthil, *Large- S expansion for quantum antiferromagnets on a triangular lattice*, J. Phys.: Condens. Matter **6** (1994) 8891.
- [4] A. L. Chernyshev and M. E. Zhitomirsky, *Erratum: Spin waves in a triangular lattice antiferromagnet: Decays, spectrum renormalization, and singularities [Phys. Rev. B **79** (2009) 144416]*, Phys. Rev. B **91** (2015) 219905.
- [5] R. Deutscher and H. U. Everts, *The $S=1/2$ Heisenberg antiferromagnet on the triangular lattice: Exact results and spin-wave theory for finite cells*, Z. Phys. B **93** (1993) 77.
- [6] R. F. Bishop, P. H. Y. Li, D. J. J. Farnell and C. E. Campbell, *Magnetic order in a spin-1/2 interpolating square-triangular Heisenberg antiferromagnet*, Phys. Rev. B **79** (2009) 174405.
- [7] Qian Li, Hong Li, Jize Zhao, Hong-Gang Luo and Z. Y. Xie, *Magnetization of the spin-1/2 Heisenberg antiferromagnet on the triangular lattice*, Phys. Rev. B **105** (2022) 184418.
- [8] W. Zheng, J. O. Fjærestad, R. R. P. Singh, R. H. McKenzie and R. Coldea, *Excitation spectra of the spin-1/2 triangular-lattice Heisenberg antiferromagnet*, Phys. Rev. B **74** (2006) 224420.
- [9] S. R. White and A. L. Chernyshev, *Neél order in square and triangular lattice Heisenberg models*, Phys. Rev. Lett. **99** (2007) 127004.
- [10] Zhenyue Zhu and Steven R. White, *Spin liquid phase of the $S = 1/2$ $J_1 - J_2$ Heisenberg model on the triangular lattice*, Phys. Rev. B **92** (2015) 041105(R).
- [11] Y. Iqbal, W.-J. Hu, R. Thomale, D. Poilblanc and F. Becca, *Spin liquid nature in the Heisenberg $J_1 - J_2$ triangular antiferromagnet*, Phys. Rev. B **93** (2016) 144411.
- [12] R. Kaneko, S. Morita and M. Imada, *Gapless spin-liquid phase in an extended spin 1/2 triangular Heisenberg model*, J. Phys. Soc. Jpn. **83** (2021) 093707.
- [13] Ahmet Keles and Erhai Zhao, *Absence of long-range order in a triangular spin system with dipolar interactions*, Phys. Rev. Lett. **120** (2018) 187202.
- [14] D. A. Huse and V. Elser, *Simple variational wave functions for two-dimensional Heisenberg Spin-1/2 antiferromagnets*, Phys. Rev. Lett. **60** (1988) 2531.
- [15] P. Sindzingre, P. Lecheminant, and C. Lhuillier, *Investigation of different classes of variational functions for the triangular and kagomé spin-1/2 Heisenberg antiferromagnets*, Phys. Rev. B **50** (1994) 3108.
- [16] S. Nakatsuji, Y. Nambu, H. Tonomura, O. Sakai, S. Jonas, C. Broholm, H. Tsunetsugu, Y. Qiu and Y. Maeno, *Spin disorder on a triangular lattice*, Science B **309** (2005) 1697.
- [17] J. M. Luttinger and L. Tisza, *Theory of dipole interaction in crystals*, Phys. Rev. **70** (1946) 954.
- [18] P. T. T. Nga and N. T. Thang, *Magnetic order of spin $S = 1$ antiferromagnetic quantum Heisenberg systems on a Bravais lattice: exact local constraint*, J. Phys.: Conf. Ser. **865** (2017) 012015.